

On the kinematics of 2D tunnel collapse in undrained clay

A. S. OSMAN^{*}, R. J. MAIR[†] and M. D. BOLTON[†]

A kinematic plastic solution has been developed for ground movements around a shallow, unlined tunnel embedded within an undrained clay layer. In this solution, the pattern of deformation around the tunnel is idealised by a simple plastic deformation mechanism. Within the boundaries of the deformation mechanism, the soil is required to shear compatibly and continuously with no relative sliding at the boundaries. The soil is regarded here as a rigid plastic (Tresca) material. The plausibility of the proposed mechanism is demonstrated by comparison with limit analysis calculations and centrifuge test results.

KEYWORDS: clays; deformation; plasticity; theoretical analysis; tunnels

Une solution plastique cinématique a été développée pour les mouvements de sol autour d'un tunnel non revêtu, de faible profondeur, creusé dans une couche d'argile non drainée. Dans cette approche, le profil de déformation autour du tunnel est idéalisé suivant le concept d'un simple mécanisme de déformation plastique. Dans les limites du mécanisme de déformation, on impose que le sol se cisaille de manière compatible et continue sans glissement relatif aux limites. Le sol est ici considéré comme un matériau plastique rigide (Tresca). La plausibilité du mécanisme proposé est démontrée par comparaison avec des calculs d'analyse de limites et les résultats d'essais au centrifuge.

INTRODUCTION

Peck (1969) summarises the most important requirements for successful design and construction in tunnels as stability, control of ground movements, and performance of linings. This paper aims to provide a simple theoretical framework for assessing the first two requirements for tunnels constructed in clays. This paper is concerned only with construction effects in clays that are presumed to remain undrained.

The upper and lower bound theorems of plasticity (Drucker *et al.*, 1952) offer a rigorous and powerful technique for estimating the collapse loads. Davis *et al.* (1980) derived plasticity solutions employing kinematic upper bounds and statically admissible lower bounds for plane-strain circular tunnels and for a two-dimensional idealisation of the tunnel heading stability in clays with constant shear strength. To obtain an upper bound to the collapse load, they developed a number of deformation mechanisms in which the soil moves as rigid blocks sliding relative to each other with displacement discontinuities at their boundaries. Davis *et al.* (1980) found that the three-variable and the four-variable mechanisms shown in Figs 1(a) and 1(b) give the lowest (i.e. the most critical) upper bounds. Sloan & Assadi (1993) developed extensive sets of upper bound and lower bound solutions for plane-strain tunnels in soils whose undrained strength varies with depth. Significant improvements on the upper bound solutions were achieved by using a more complex seven-variable mechanism (Fig. 1(c)). Sloan & Assadi (1993) also improved both upper bound and lower bound calculations using numerical limit analysis. In this technique, rigorous upper and lower bound collapse loads are found numerically by linear programming methods, while spatial discretisation (lower bound stresses) and interpolation of the field variables (upper bound velocities) are accomplished using finite element methods.

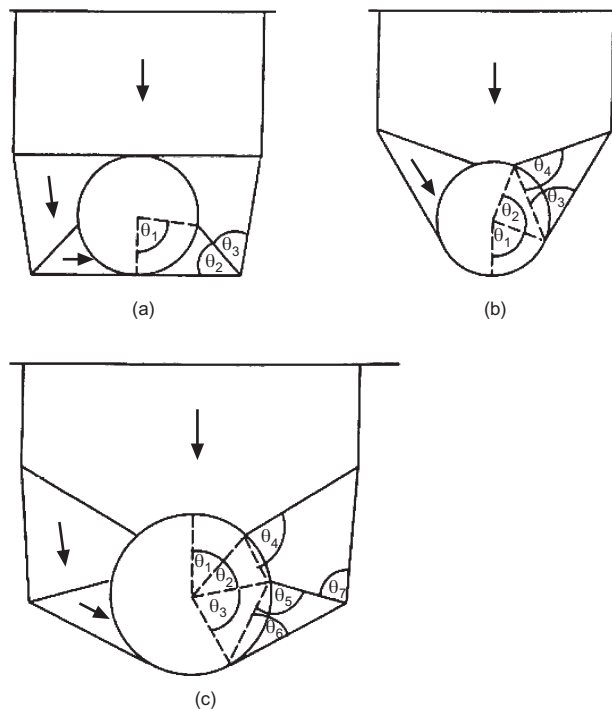


Fig. 1. Upper bound mechanisms used in the stability calculations for shallow tunnels: (a) three-variable mechanism (Davis *et al.*, 1980); (b) four-variable mechanism (Davis *et al.*, 1980); (c) seven-variable mechanism (Sloan & Assadi 1993)

Although the rigid block mechanisms mentioned above produced reasonable estimates for collapse loads, these mechanisms do not attempt to replicate the actual settlement profile of the ground surface, and the geometry of the mechanisms does not necessarily represent the extent of the displacement field around the tunnels or the variation of the settlement trough with depth. In the following sections, the authors will demonstrate that the upper bound theorem coupled with a more realistic continuous deformation

Manuscript received 3 February 2006; revised manuscript accepted 19 September 2006.

Discussion on this paper closes on 1 May 2007, for further details see p. ii.

^{*} School of Engineering, Durham University, UK.

[†] Department of Engineering, University of Cambridge, UK.

mechanism can not only offer a reasonable assessment for collapse, but also replicates some of the features observed in centrifuge tests of tunnelling in undrained clay.

PLASTIC DEFORMATION MECHANISM

Peck (1969) suggested that the shape of the surface settlement trough developing during tunnel construction is reasonably well represented by a Gaussian distribution as shown in Fig. 2. This suggestion is consistent with a considerable amount of field data of surface settlement profiles above tunnels in clays.

The surface settlement s is defined as

$$s = s_m \exp \left[-\frac{1}{2} \left(\frac{x}{i} \right)^2 \right] \tag{1}$$

where s_m is the maximum surface settlement, which occurs above the tunnel centreline. The width of the surface settlement profile is defined by the parameter i , which is the distance from the tunnel centreline to the point of inflexion of the trough (shown in Fig. 2).

The volume of the surface settlement trough (per metre length of tunnel), V_s , is obtained from integration of equation (1), and is given by

$$V_s = \sqrt{2\pi} i s_m \tag{2}$$

In practice, the parameter i is related to the depth of the centre of the tunnel z_0

$$i = K z_0 \tag{3}$$

Rankin (1988) and Mair & Taylor (1997) showed that $K = 0.5$ is reasonably consistent with field measurements of surface settlement above tunnels in clays for a large number of case histories.

Figure 3 shows a new plastic deformation mechanism for a tunnel in undrained clay proposed in this paper. Within the boundary of the deformation mechanism the soil is deforming compatibly following a Gaussian distribution. Outside this mechanism the soil is assumed to be rigid.

By analogy with equations (2) and (3), subsurface settlement profiles can be defined using a trough width parameter i_z that is a function of depth z ,

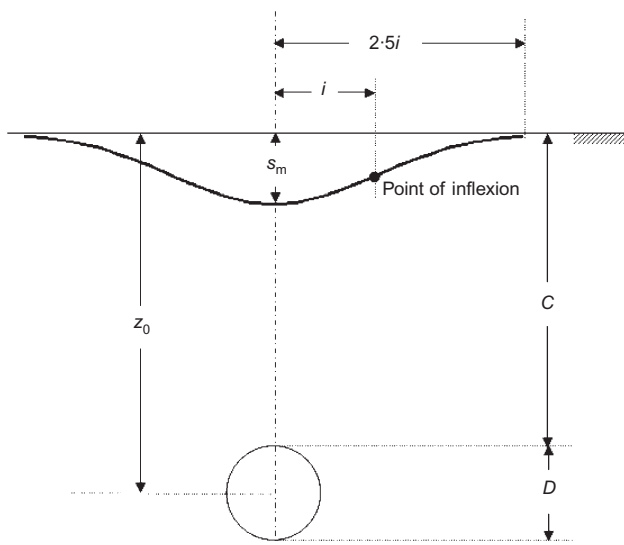


Fig. 2. Surface settlement profile above tunnels

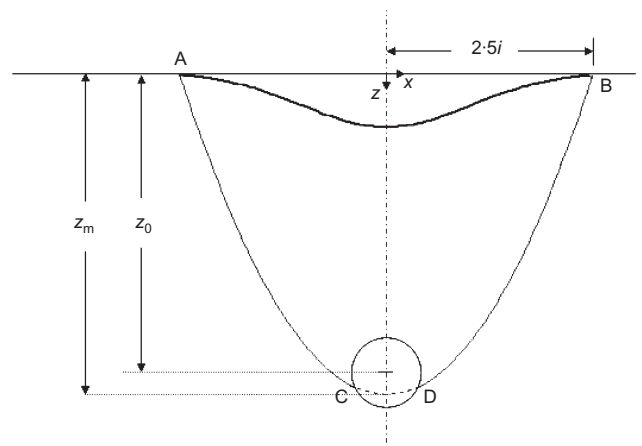


Fig. 3. Plastic deformation mechanism for tunnels in clay

$$i_z = K_z z_0 \tag{4}$$

where

$$K_z = 0.5 \left(1 - \frac{z}{z_m} \right)^\alpha \tag{5}$$

and where z_m is the depth below the ground surface of the point of intersection of the extension of the boundary AC (and BD) with the extension of the vertical centreline of the tunnel, and α is a constant controlling the vertical curvature of the outer boundary of the mechanism shown in Fig. 3.

Note that for the subsidence at the ground surface $z = 0$, so that $K_z = 0.5$, which is consistent with the Rankin formula (equation (3)). Also, at $z = z_m$, the width i_z is correctly calculated at zero.

The proposed mechanism shown in Fig. 3 implies zero ground movement at the boundaries AC and BD, so it is necessary to adjust the Gaussian curve accordingly. The vertical displacement v is therefore given by

$$v = \frac{A s_m}{2 K_z} \left\{ \exp \left[-\frac{1}{2} \left(\frac{x}{i_z} \right)^2 \right] - \exp \left[-\frac{B^2}{2} \right] \right\} \tag{6}$$

where A and B are constants.

It is commonly assumed that the total half-width of the surface settlement trough is about $2.5 i$ (Mair *et al.*, 1993). Therefore B can be taken to be 2.5 to achieve zero displacement at $x = 2.5 i_z$. Accordingly, A must take the value 1.046 to achieve $v = s_m$ at $z = 0$ and $x = 0$.

If there is no volume change, the following condition should be satisfied.

$$\frac{\partial u}{\partial x} + \frac{\partial v}{\partial z} = 0 \tag{7}$$

where u is the horizontal displacement.

The horizontal displacement component u can then be found by substituting equation (6) in equation (7) and integrating.

$$u = -\frac{\alpha A s_m x}{2 K_z (z_m - z)} \left\{ \exp \left[-\frac{1}{2} \left(\frac{x}{i_z} \right)^2 \right] - \exp \left[-\frac{B^2}{2} \right] \right\} \tag{8}$$

Equation (8) implies that the maximum horizontal movement occurs at the point of inflexion of the trough. This is consistent with field observations reported by Attewell (1978), as shown in Fig. 4.

Strains can be found from the first derivative of displacements. Applying plane-strain conditions,

$$\begin{aligned} \epsilon_x &= \frac{\partial u}{\partial x} \\ \epsilon_z &= \frac{\partial v}{\partial z} \\ \gamma_{xz} &= \frac{\partial u}{\partial z} + \frac{\partial v}{\partial x} \end{aligned} \tag{9}$$

The engineering shear strain ϵ_s is then given by

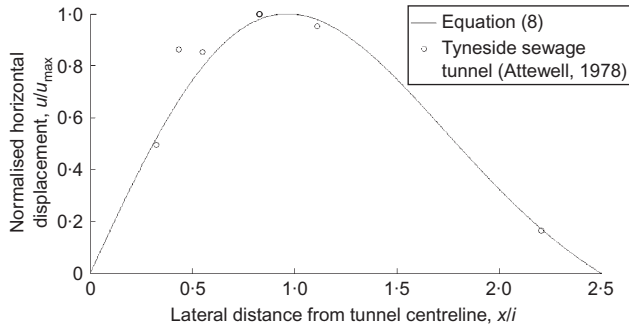


Fig. 4. Normalised horizontal displacement profile

$$\epsilon_s = \sqrt{(\epsilon_x - \epsilon_z)^2 + \gamma_{xz}^2} \tag{10}$$

Detailed derivations are given in Appendix 1.

STABILITY ANALYSIS

In plasticity, the geometry of the plastic deformation mechanism is selected to obtain the least upper bound to the

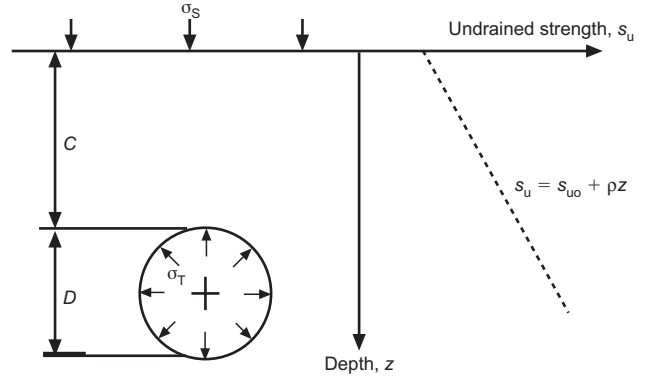


Fig. 5. Idealisation of unlined plane-strain tunnel in clay

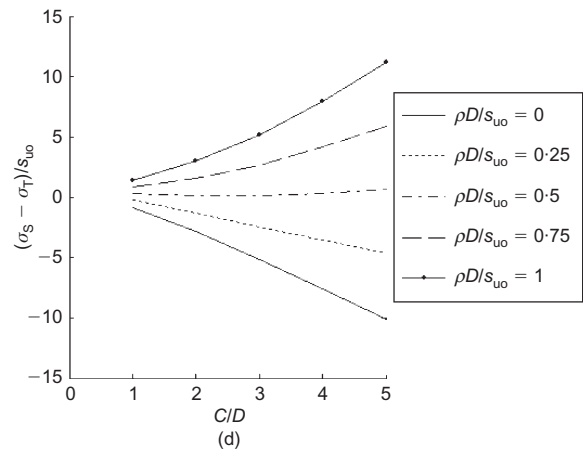
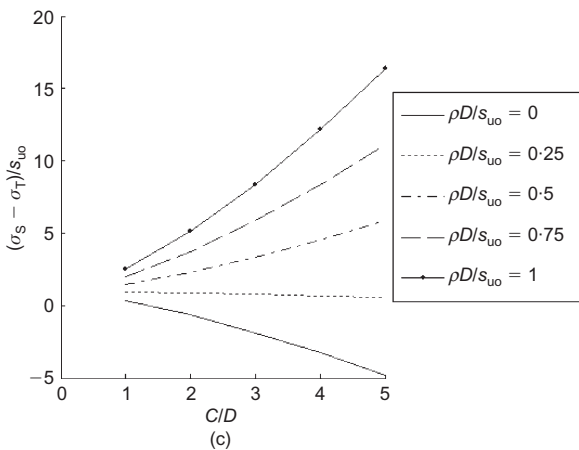
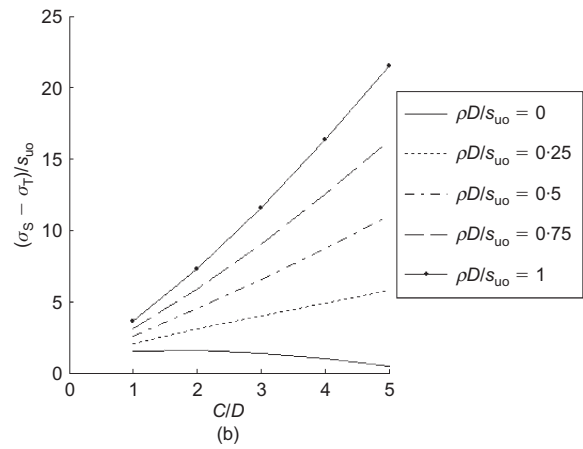
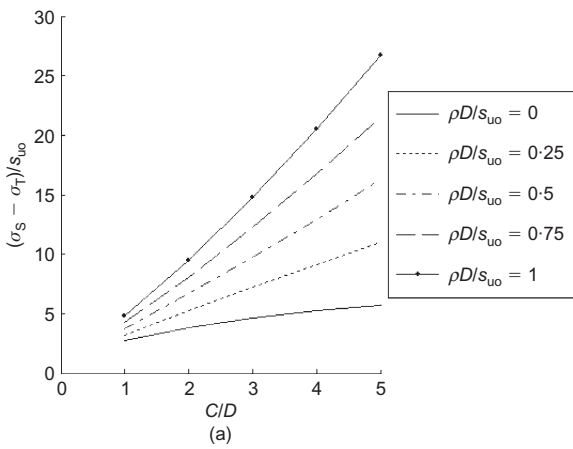


Fig. 6. Stability bounds for circular tunnels: (a) $\gamma D/s_{u0} = 0$; (b) $\gamma D/s_{u0} = 1$; (c) $\gamma D/s_{u0} = 2$; (d) $\gamma D/s_{u0} = 3$

collapse load calculated via the work equation. Work by external forces (or gravity forces) due to a small displacement increment in the assumed mechanism is equated to the internal dissipation of energy in the plastically deforming regions of the mechanism (Chen, 1975).

From the proposed plastic deformation mechanism shown in Fig. 3, the virtual plastic work in distributed shearing balances the virtual loss of potential energy and the work done by tunnel pressure σ_T and surcharge load on the ground surface σ_S (shown in Fig. 5). Since there is no volume change, the decrease in area of the tunnel must equal the area of ground loss at the surface. Therefore the work done per unit length of tunnel by the pressures should be $(\sigma_S - \sigma_T)$ multiplied by the displaced area. The work equation in plane strain for a Tresca material is therefore given by

$$\int_{-1.25z_0}^{1.25z_0} (\sigma_S - \sigma_T) \delta v_{z=0} dx + \int_{Area} \gamma \delta v dArea = \int_{Area} s_u \delta \epsilon_s dArea \tag{11}$$

where s_u is the undrained shear strength, γ is the unit weight of the soil, δv is the vertical displacement increment, and $Area$ is the area of the mechanism shown in Fig. 3.

The stability of the tunnels is often expressed by the stability number N_c , which is defined by (Broms & Bennermark, 1967)

$$N_c = \frac{\sigma_S + \gamma z_0 - \sigma_T}{s_{u,T}} \tag{12}$$

where $s_{u,T}$ is the undrained shear strength at the tunnel axis level.

The undrained strength profile can vary linearly with depth according to

$$s_u = s_{u0} + \rho z \tag{13}$$

where s_{u0} is the undrained strength at the ground surface, and $\rho = ds_u/dz$ is the rate of change of undrained strength with depth. This creates an additional dimensionless group $\rho D/s_{u0}$ and increases the shear strength at the tunnel axis to $[s_{u0} + \rho(C + D/2)]$. Therefore the stability number N_c in these circumstances can be rewritten as

$$N_c = \left[\frac{\sigma_S - \sigma_T}{s_{u0}} + \frac{\gamma D}{s_{u0}} \left(\frac{C}{D} + \frac{1}{2} \right) \right] \times \left[\frac{1}{1 + (\rho D/s_{u0})(C/D + 1/2)} \right] \tag{14}$$

where C is the depth of cover, and D is the tunnel diameter.

In many design situations, the quantities $\gamma D/s_{u0}$, $\rho D/s_{u0}$ and C/D are known, and the problem can be regarded as finding the critical (lowest) value of $(\sigma_S - \sigma_T)/s_{u0}$.

Figure 6 shows the values of $(\sigma_S - \sigma_T)/s_{u0}$ calculated from the proposed plastic deformation mechanism for different values of $\gamma D/s_{u0}$, $\rho D/s_{u0}$ and C/D . The optimum geome-

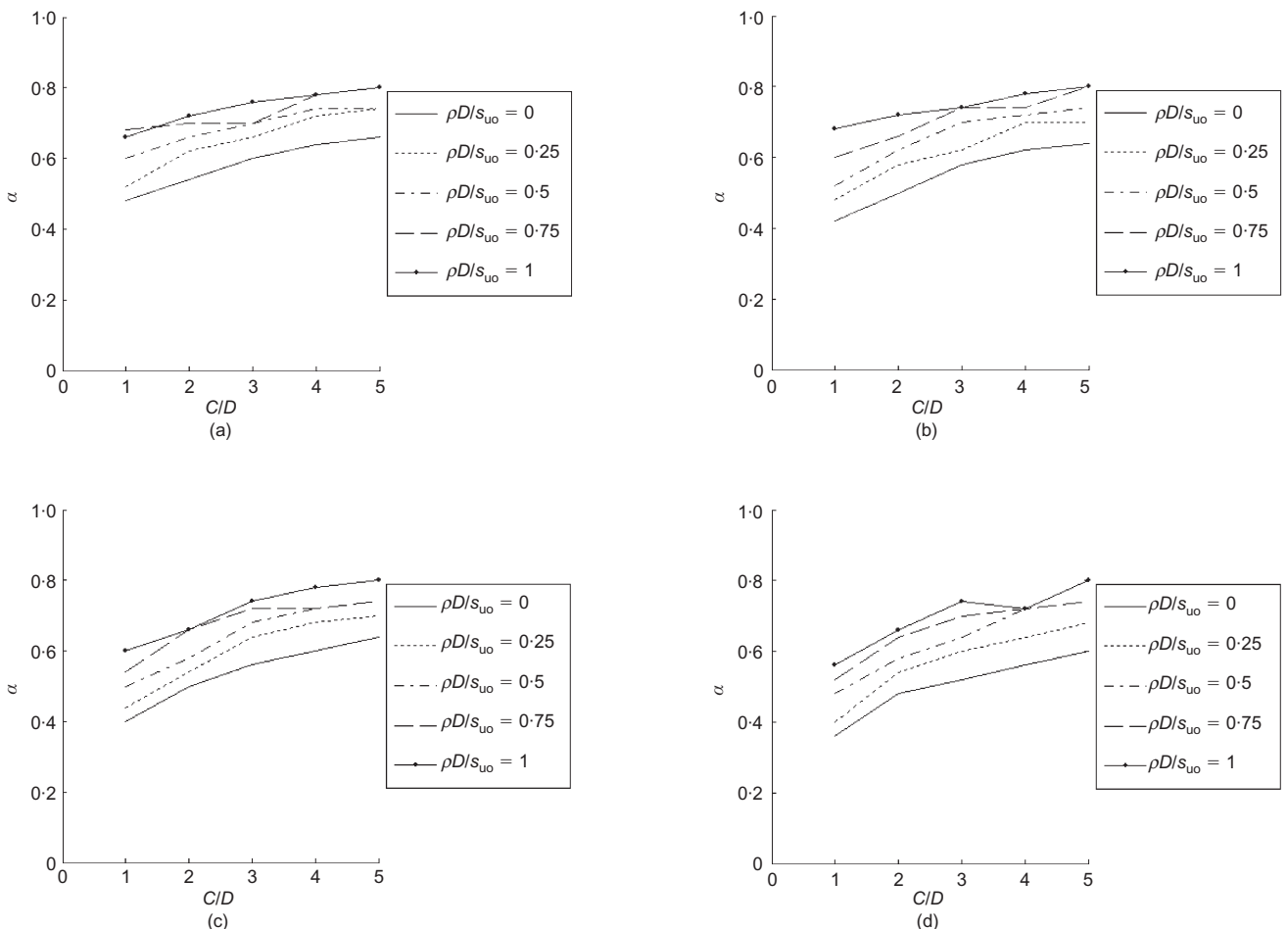


Fig. 7. Values of α in equation (5): (a) $\gamma D/s_{u0} = 0$; (b) $\gamma D/s_{u0} = 1$; (c) $\gamma D/s_{u0} = 2$; (d) $\gamma D/s_{u0} = 3$

try of the mechanism that gives the least upper bound is obtained by iterating on the depth z_m and exponent α in equation (5), which govern the shape of the side of the mechanism (Fig. 3). The values of z_m and α are restricted by the fact that points C and D in Fig. 3 should lie at the tunnel circumference in order to satisfy the undrained condition, because the decrease in area of the tunnel must equal the area of ground loss at the surface. The optimum values of z_m and exponent α that give the least upper bound are given in Figs 7 and 8 respectively. The value of α is found to vary from about 0.4 at $C/D = 1$ in the case of strength increase with depth ($\rho D/s_{uo} = 1$) to about 0.8 at $C/D = 5$ in the case of soil with constant shear strength ($\rho D/s_{uo} = 0$). The depth z_m of the point of intersection of the side boundaries (AC and BD) with the vertical centreline of the tunnel (Fig. 3) lies at a distance of about 0.45 to 0.82 times the tunnel radius below the centre of the tunnel circle, generally increasing as C/D increases.

The bold entries in Table 1 show the value of $(\sigma_S - \sigma_T)/s_{uo}$ calculated from the proposed two-variable plastic deformation mechanism of distributed shear shown in Fig. 3 using equations (7)–(11). Other entries indicate upper bound solutions proposed by Sloan & Assadi (1993) and based on a seven-variable rigid block mechanism (Fig. 1) and on their finite element formulation. The bold italic values indicate where the proposed mechanism predicts the least upper bounds for cases of deep tunnels ($C/D \geq 4$). However, it slightly overestimates the collapse load for the case of very shallow tunnels ($C/D = 1$) embedded in soft soil, $\gamma D/s_{uo} = 3$. Results for two extreme values of $\gamma D/s_{uo}$ with a strength

profile of $\rho D/s_{uo} = 0.5$ are plotted in Fig. 9. The proposed mechanism predicts $(\sigma_S - \sigma_T)/s_{uo}$ values consistent with the best of Sloan & Assadi's calculations.

CONSISTENCY OF THE PROPOSED PLASTIC DEFORMATION MECHANISM

To assess the ability of the proposed distributed shear mechanism to predict the stability of tunnels in practice and to represent real deformations around tunnels, it is necessary to compare theoretical predictions with observed behaviour. Although it is always valuable to be able to compare theoretical analyses with full-scale observations, it is often difficult to obtain all the required information about the soil, the structure, its loads and settlements, and the drainage conditions. Many of these uncertainties are avoided by observation of the behaviour of closely monitored scale models using well-documented soils. The centrifuge experiments conducted by Mair (1979) are a valuable dataset for this purpose.

The centrifuge tests were carried out using the Cambridge Geotechnical Centrifuge. Model tunnels were constructed in soft clay and tested at accelerations of 75g and 125g respectively to establish the internal consistency of the method. Tunnel behaviour was observed as compressed air support within the tunnels was steadily reduced until failure occurred. Two series of centrifuge tests on plane-section tunnels in clay were conducted. The first series was in clay with constant undrained shear strength with depth. In the second series, the clay was brought into equilibrium

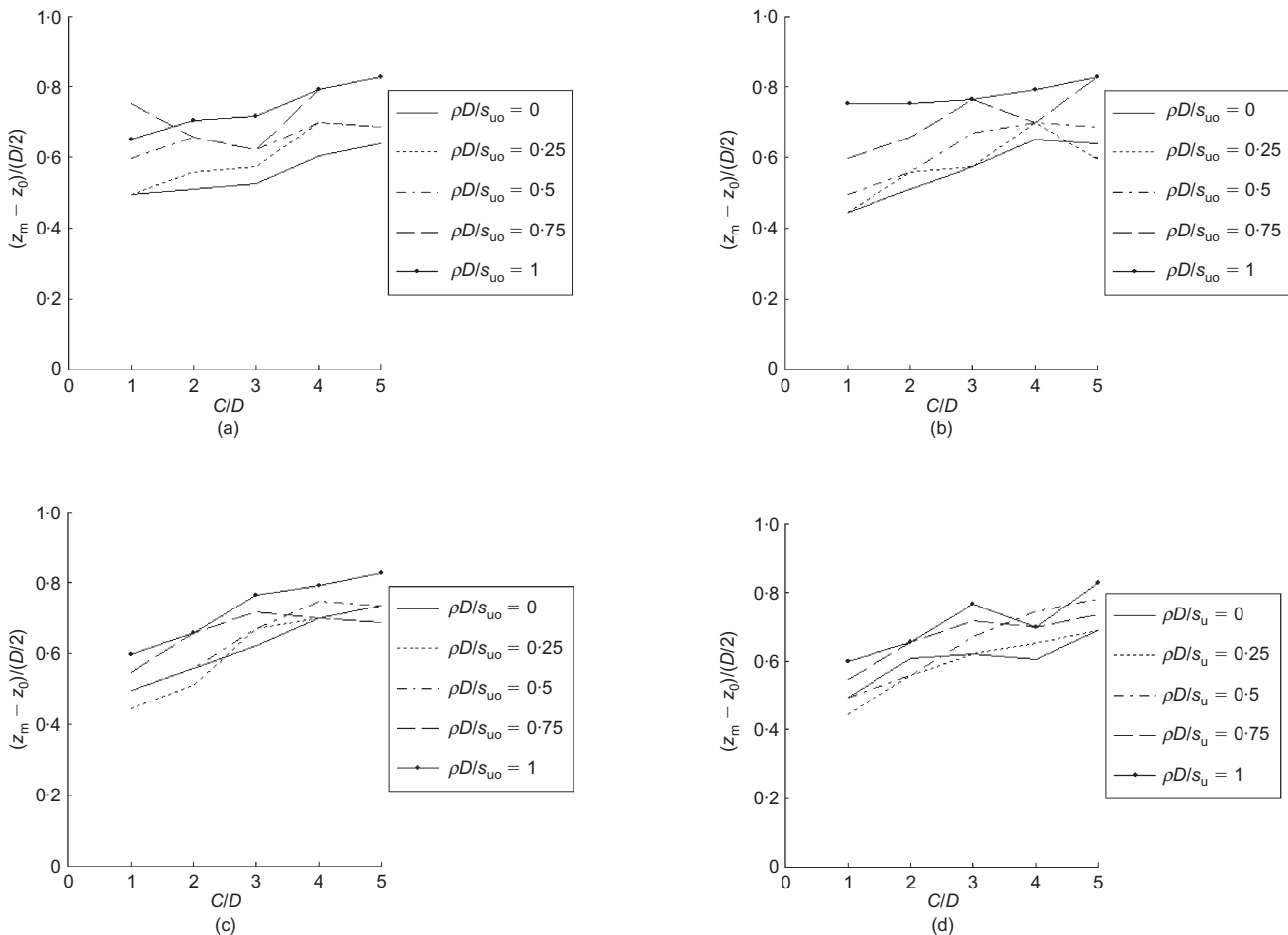


Fig. 8. Values of z_m in equation (5): (a) $\gamma D/s_{uo} = 0$; (b) $\gamma D/s_{uo} = 1$; (c) $\gamma D/s_{uo} = 2$; (d) $\gamma D/s_{uo} = 3$

Table 1. Stability bounds of shallow tunnels in clay

$\frac{C}{D}$	$\frac{\rho D}{s_{uo}}$	$\frac{\sigma_s - \sigma_T}{s_{uo}}$							
		$\frac{\gamma D}{s_{uo}} = 0$		$\frac{\gamma D}{s_{uo}} = 1$		$\frac{\gamma D}{s_{uo}} = 2$		$\frac{\gamma D}{s_{uo}} = 3$	
1	0	2.55	2.70	1.37	1.54	0.15	0.36	-1.12	-0.83
	0.25	3.05	3.23	1.91	2.08	0.73	0.92	-0.47	-0.25
	0.5	3.53	3.75	2.41	2.61	1.26	1.46	0.10	0.31
	0.75	4.01	4.26	2.89	3.13	1.76	1.99	0.62	0.84
	1	4.46	4.76	3.35	3.64	2.24	2.51	1.11	1.37
2	0	3.68	3.84	1.41	1.62	-0.91	-0.60	-3.28	-2.85
	0.25	5.10	5.27	2.89	3.08	0.65	0.89	-1.61	-1.32
	0.5	6.48	6.68	4.29	4.51	2.08	2.33	-0.14	0.13
	0.75	7.85	8.07	5.66	5.91	3.46	3.74	1.26	1.56
	1	9.20	9.47	7.02	7.31	4.83	5.15	2.64	2.98
3	0	4.51	4.63	1.18	1.39	-2.20	-1.86	-5.63	-5.14
	0.25	7.11	7.19	3.85	3.99	0.56	0.78	-2.72	-2.45
	0.5	9.62	9.72	6.39	6.53	3.15	3.34	-0.11	0.14
	0.75	12.10	12.24	8.88	9.06	5.66	5.87	2.42	2.68
	1	14.57	14.75	11.34	11.57	8.14	8.39	4.92	5.21
4	0	5.17	5.24	0.80	0.99	-3.61	-3.28	-8.08	-7.56
	0.25	9.15	9.09	4.86	4.88	0.56	0.66	-3.77	-3.57
	0.5	12.99	12.91	8.73	8.71	4.46	4.51	0.18	0.31
	0.75	16.80	16.72	12.56	12.53	8.30	8.33	4.03	4.14
	1	20.60	20.52	16.36	16.34	12.11	12.15	7.85	7.97
5	0	5.67*	5.73	0.30*	0.48	-5.30*	-4.80	-10.60*	-10.10
	0.25	11.25	11.02	5.94	5.80	0.61	0.58	-4.74	-4.65
	0.5	16.59	16.26	11.30	11.06	6.01	5.85	0.70	0.64
	0.75	21.89	21.50	16.62	16.30	11.33	11.09	6.04	5.90
	1	27.17	26.72	21.91	21.53	16.63	16.33	11.35	11.15

Bold entries indicate upper bound from the distributed shear mechanism. Bold italic entries indicate the least upper bounds from the distributed shear mechanism. Regular entries indicate upper bounds from Sloan & Assadi (1993) based on seven-variable rigid block mechanism and on finite element formulations. Finite element values are followed by the symbol *.

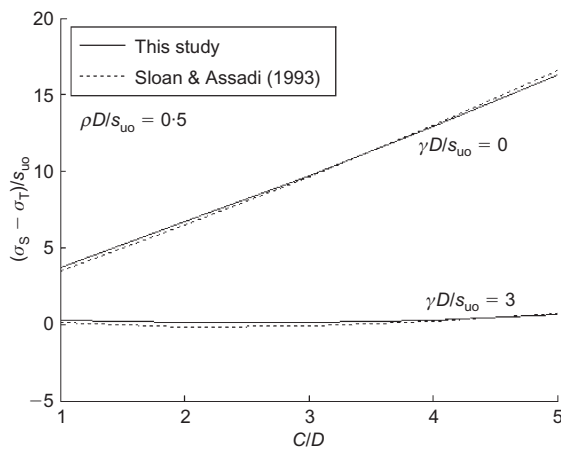


Fig. 9. Comparison of stability bounds for circular tunnel in soil whose undrained strength varies with depth ($\rho D/s_{uo} = 0.5$)

in an overconsolidated state on the centrifuge so that strength increased with depth. In each case, compressed air was used to support the tunnel as the centrifuge acceleration was applied, and was reduced incrementally to simulate tunnel excavation. Details of the centrifuge tests used in the validation of the proposed deformation mechanism are

shown in Table 2. Fig. 10 shows the undrained strength profile of the second series. Tests 2DT and 2DU were designed to model tests 2DP and 2DV respectively, at different scale.

Surface settlement profile

Normalised surface settlement (s/s_m) plotted against normalised distance from tunnel centreline (x/D) is presented in Fig. 11. The surface settlement s is calculated from equation (6) ($s = v_{z=0}$). This figure shows that the shape and the width of the settlement troughs were very similar at different stages of both tests 2DV and 2DU. A unique profile was also obtained in tests 2DP and 2DT. The settlement troughs shown in this figure do indeed closely approximate the modified Gaussian curve as given by equation (6). The variation of the width of the settlement trough with depth of tunnel axis is shown in Fig. 12. All the centrifuge test results fall within the limits suggested by Peck (1969) and agree reasonably with the empirical expression of Clough & Schmidt (1981). The test results also compared reasonably well for the width of the surface settlement trough given by equations (4) and (5). However, these equations might overestimate the width of the settlement trough for deeper tunnels ($z_0/D > 4$). These results imply that displacements around shallow tunnels at any level of tunnel pressure could be represented reasonably by the deformation mechanism shown in Fig. 2.

Table 2. Centrifuge tests, conducted by Mair (1979), used in the validation

Test no.	Cover to diameter ratio, C/D	Laboratory consolidation pressure: kPa	Centrifuge acceleration: g		Tunnel diameter, D : mm	Undrained shear strength, s_u
			Acceleration at base of model	Average acceleration in model		
Series I						Constant undrained shear strength, $s_u = 26$ kPa
2DB	1.2	171	75	71	60	
2DD	2.8	171	75	71	60	
2DE	0.8	171	75	71	60	
2DH	1.8	171	75	71	60	
2DI	2.3	171	75	71	60	
2DK	2	171	75	71	60	
Series II						Varies with depth (see Fig. 8)
2DP	1.67	171	75	71	60	
2DV	3.11	171	75	71	60	
2DT	1.67	171	125	119	36	
2DU	3.11	171	125	119	36	

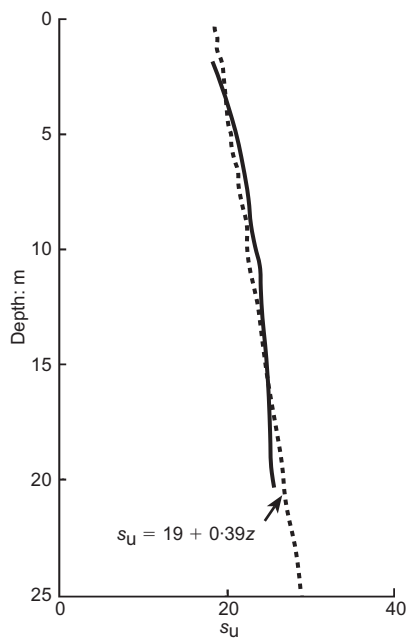


Fig. 10. Undrained strength s_u profile in Series II centrifuge tests (Mair, 1979)

Width of subsurface settlement profile

Mair *et al.* (1993) studied data both from field measurements of tunnels in clay and from centrifuge tests, and suggested that the values of the trough width parameter i_z derived from subsurface settlement measurements can best be fitted by

$$\frac{i_z}{z_0} = 0.175 + 0.325 \left(1 - \frac{z}{z_0} \right) \tag{15}$$

Figure 13 shows values of the trough width parameter i_z derived from subsurface settlement measurements from two centrifuge tests on tunnels in soft clay (2DP and 2DV) by Mair (1979), plotted against depth z ; both i_z and z have been normalised by the depth of the tunnel, z_0 . The trough width

parameter i_z derived from the distributed shear mechanism proposed in this paper, using equations (4) and (5), and from equation (15) of Mair *et al.* (1993), is also shown in Fig. 13. The same values of depth z_m and exponent α that gave the optimised upper bound (see Table 3) also provide accurate deformation profiles prior to collapse.

It is worth mentioning that Mair *et al.* (1993) defined the parameter K as the width parameter i_z divided by the distance above the tunnel centre ($z_0 - z$). This definition is different from the authors' expressions (equation (5)). Fig. 14 compares the values of $i_z/(z_0 - z)$ obtained from upper bound calculations and from the empirical expression of Mair *et al.* (1993) (equation 15) with centrifuge test results. The good agreement suggests that the upper bound theorem coupled with distributed shear deformation mechanisms can provide a sound theoretical framework for estimating the subsurface settlement trough.

Displacement vector patterns

The displacement vectors measured for tests 2DP and 2DV close to collapse are shown in Figs 15 and 16 respectively, together with the vector patterns derived from the distributed shear plastic deformation mechanism. A degree of asymmetry in deformation pattern is evident for both tests. Mair (1979) concluded from surface settlement profiles at different level tunnel support pressure that the asymmetry appears to develop only close to collapse. The deformation mechanism observed from displacement plots reveals significant inward displacement at the tunnel crown and shoulders, while much smaller movement is observed at the tunnel springings and inverts as required by the plastic deformation mechanism shown in Fig. 3.

CONCLUSIONS

This paper demonstrates the usefulness of the upper bound theorem not only in assessing the stability of shallow tunnels in undrained clay, but also in providing a reasonable approximation of the deformation pattern. The width of subsurface settlement trough can be determined analytically from upper bound calculations in which a plastic deformation mechanism with distributed shear is incorporated.

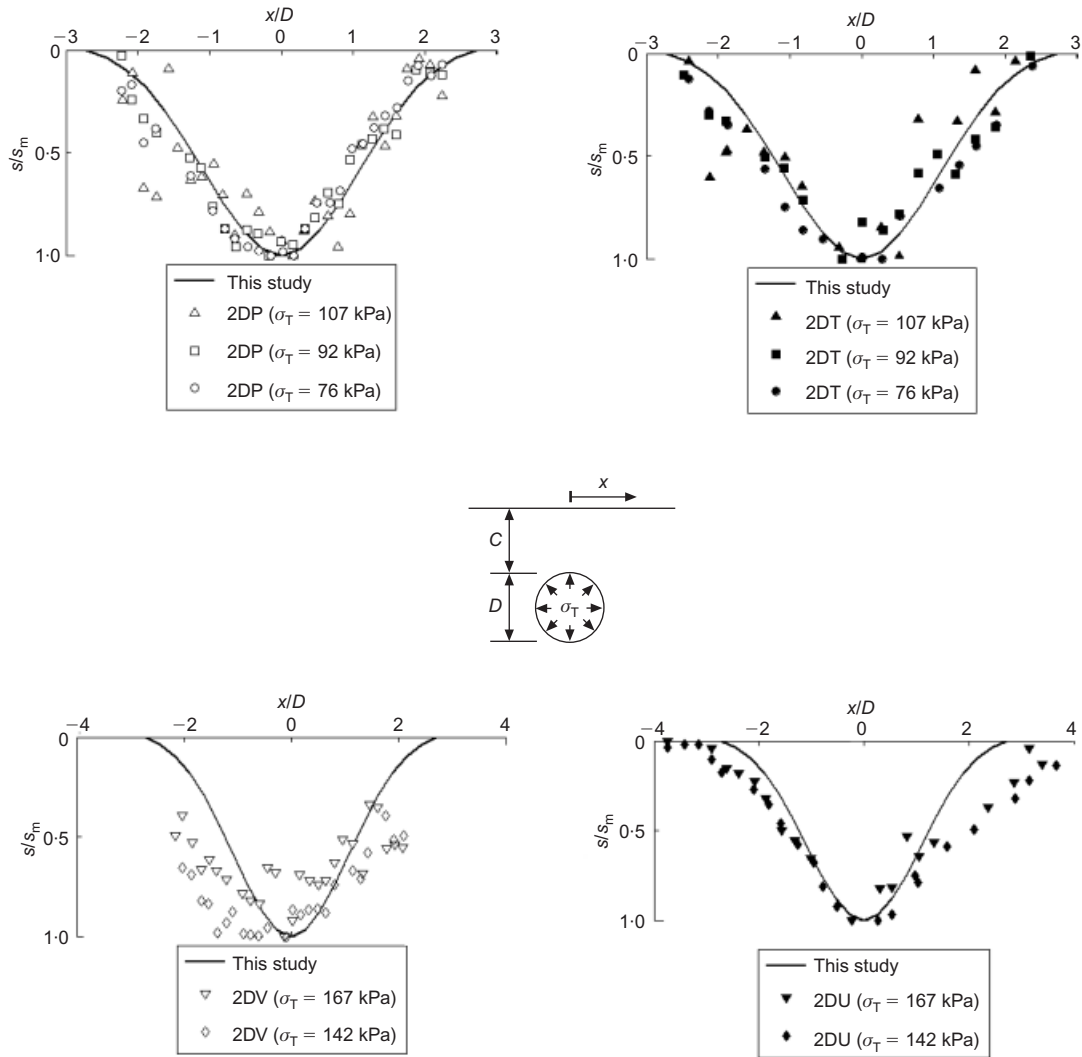


Fig. 11. Surface settlement profiles at different stages of centrifuge tests (Mair, 1979)

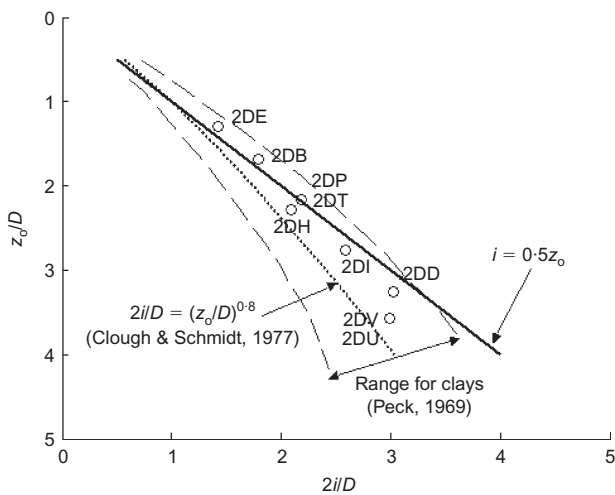


Fig. 12. Variation of surface settlement trough width with depth of tunnel axis in centrifuge tests (Mair, 1979)

Grant GR/T 18660/01. The authors would like to thank Dr David White for his useful discussion and for his constructive comments.

APPENDIX 1. STRAIN COMPONENTS

By substituting equations (4) and (5) in equation (7), the vertical displacement can be written as

$$v = \frac{As_m(z_m)^\alpha}{(z_m - z)^\alpha} \left(\exp \left\{ -2 \left[\frac{x(z_m)^\alpha}{(z_m - z)^\alpha z_0} \right]^2 \right\} - \exp \left(-\frac{B^2}{2} \right) \right) \tag{16}$$

ACKNOWLEDGEMENTS

The authors acknowledge the support of the Engineering and Physical Sciences Research Council (EPSRC): Platform

By substituting equations (4) and (5) in equation (8), the horizontal displacement can be written as

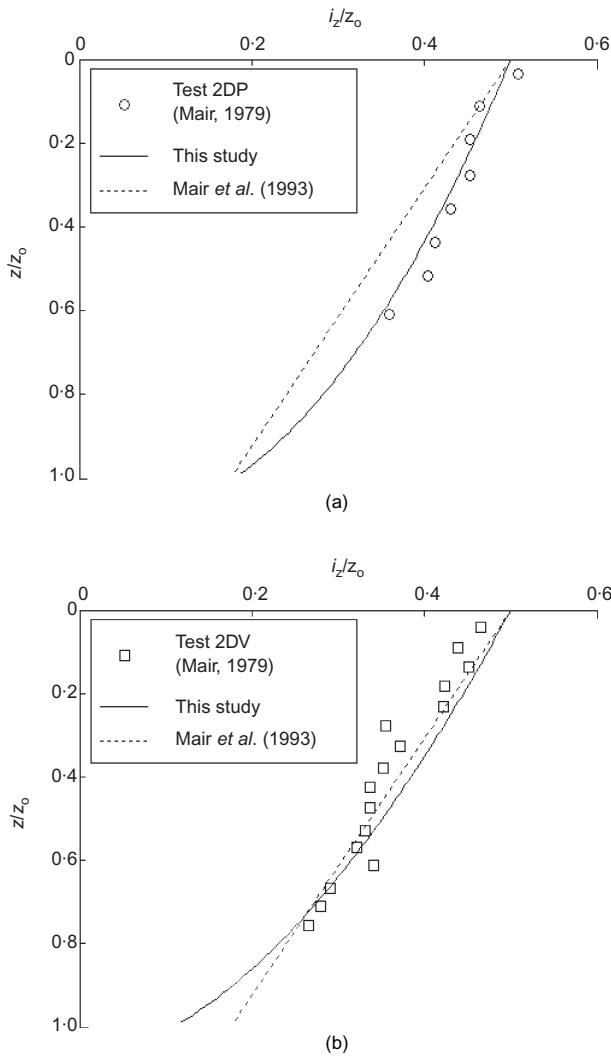


Fig. 13. Variation of subsurface settlement trough width parameter with depth for tunnels in clays: (a) centrifuge model 2DP; (b) centrifuge model 2DV

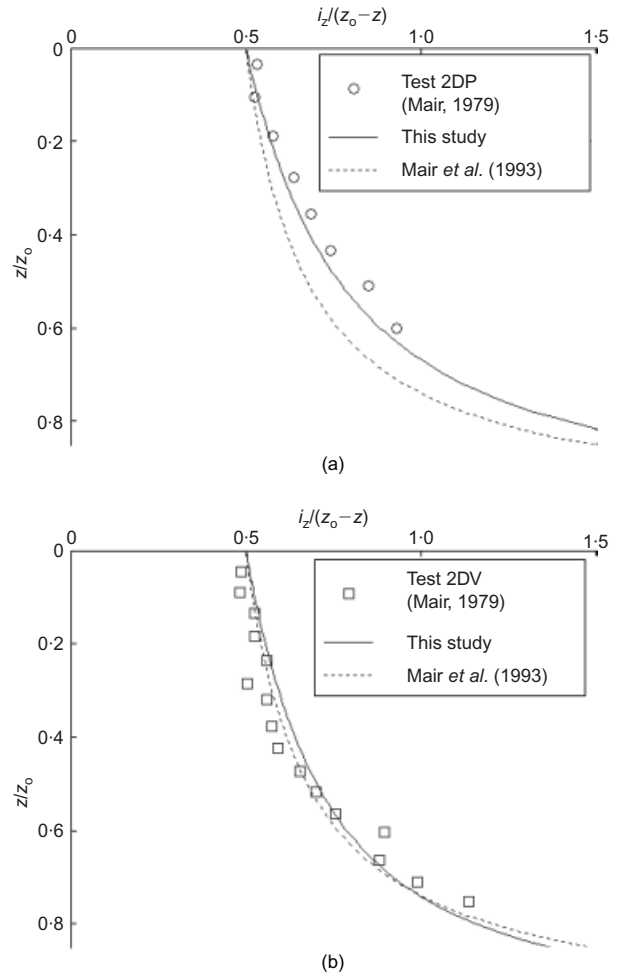


Fig. 14 Variation of $i_z/(z_0 - z)$ with depth for subsurface settlement profiles above tunnels in clays

$$u = -\frac{\alpha A s_m (z_m)^\alpha x}{(z_m - z)^{\alpha+1}} \left(\exp \left\{ -2 \left[\frac{x(z_m)^\alpha}{(z_m - z)^\alpha z_0} \right]^2 \right\} - \exp \left(-\frac{B^2}{2} \right) \right) \quad (17)$$

$$\begin{aligned} \varepsilon_z &= \frac{\partial v}{\partial z} \\ &= \frac{\alpha A s_m (z_m)^\alpha}{(z_m - z)^{\alpha+1}} \left(\left\{ 1 - 4 \left[\frac{x(z_m)^\alpha}{(z_m - z)^\alpha z_0} \right]^2 \right\} \right. \\ &\quad \times \exp \left\{ -2 \left[\frac{x(z_m)^\alpha}{(z_m - z)^\alpha z_0} \right]^2 \right\} - \exp \left(-\frac{B^2}{2} \right) \left. \right) \end{aligned} \quad (18)$$

The strain in the vertical direction, ε_z , is therefore

The strain in the horizontal direction (x -direction) is found by differentiating the horizontal displacement with respect to x .

Table 3. Stability analysis of centrifuge tests conducted by Mair (1979)

Test no.	$\frac{\gamma D}{s_{uo}}$	$\frac{\rho D}{s_{uo}}$	$\frac{\sigma_s - \sigma_T}{s_{uo}}$	α	$\frac{z_m - z_0}{D/2}$
2DP	3.5649	0.0874	-2.80	0.45	0.58
2DT	3.5649	0.0874	-2.80	0.45	0.58
2DV	3.5649	0.0874	-6.29	0.55	0.62
2DU	3.5649	0.0874	-6.29	0.55	0.62

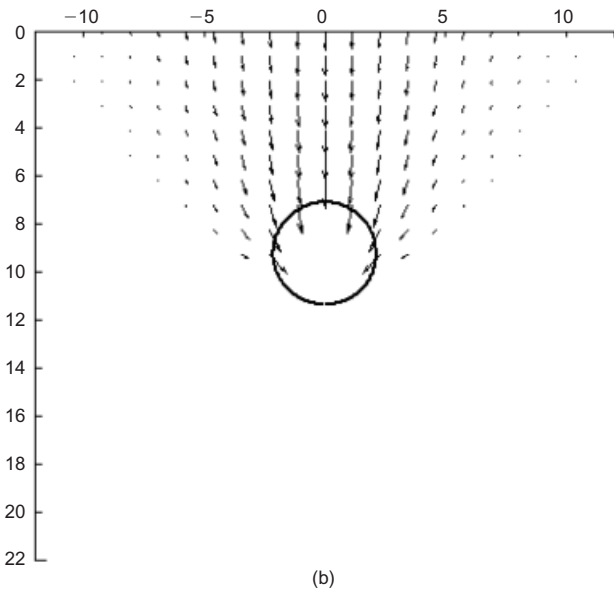
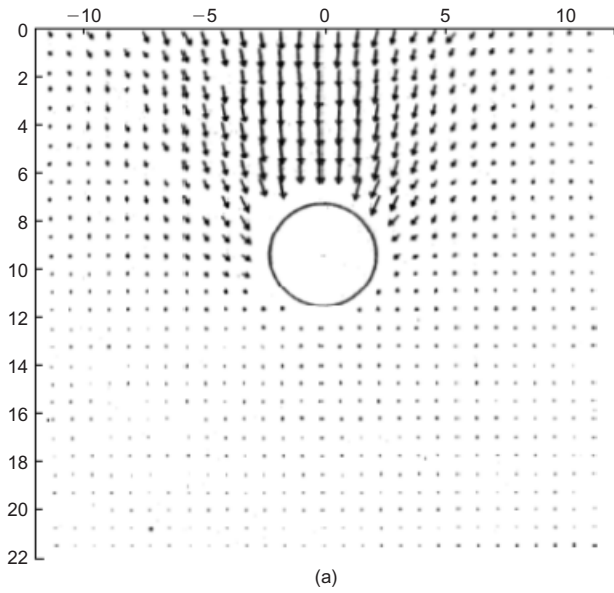


Fig. 15. Displacement vectors just before collapse in test 2DP: (a) observed displacement vectors ($\sigma_T = 66$ kPa); (b) calculated displacement vector patterns

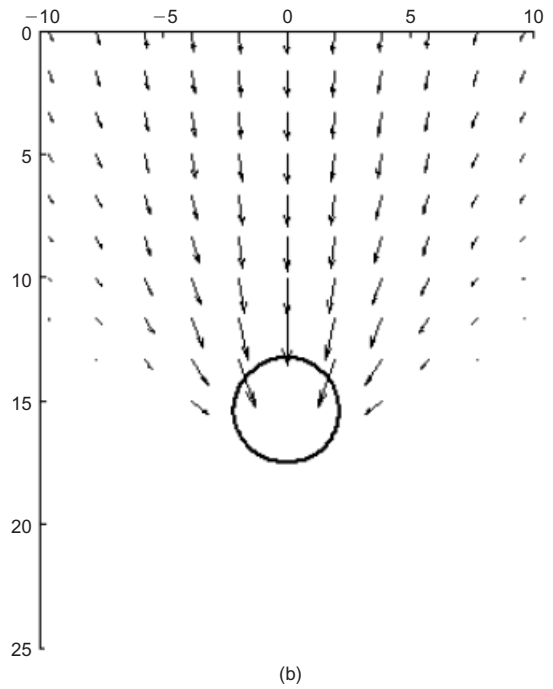
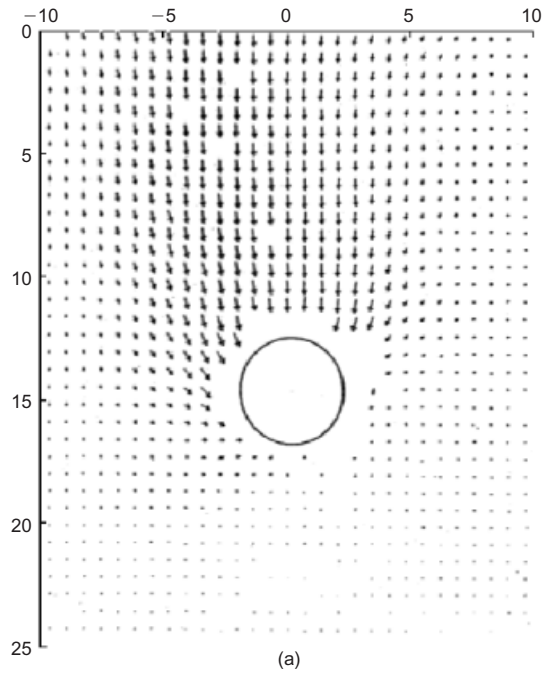


Fig. 16. Displacement vectors just before collapse in test 2DV: (a) observed displacement vectors ($\sigma_T = 107$ kPa); (b) calculated displacement vector patterns

$$\begin{aligned} \epsilon_x &= \frac{\partial u}{\partial x} \\ &= -\frac{\alpha A s_m (z_m)^\alpha}{(z_m - z)^{\alpha+1}} \left(\left\{ 1 - 4 \left[\frac{x(z_m)^\alpha}{(z_m - z)^\alpha z_0} \right]^2 \right\} \right. \\ &\quad \left. \times \exp \left\{ -2 \left[\frac{x(z_m)^\alpha}{(z_m - z)^\alpha z_0} \right]^2 \right\} - \exp \left(-\frac{B^2}{2} \right) \right) \end{aligned} \quad (19)$$

Differentiating equation (16) with respect to x gives

$$\frac{\partial v}{\partial x} = -\frac{4 A s_m x (z_m)^{3\alpha}}{(z_m - z)^{3\alpha} (z_0)^2} \exp \left\{ -2 \left[\frac{x(z_m)^\alpha}{(z_m - z)^\alpha z_0} \right]^2 \right\} \quad (20)$$

Differentiating equation (17) with respect to z gives

$$\begin{aligned} \frac{\partial u}{\partial z} &= -\frac{\alpha(1 + \alpha) A s_m (z_m)^\alpha x}{(z_m - z)^{\alpha+2}} \times \left(\left\{ 1 - \frac{4\alpha}{1 + \alpha} \left[\frac{x(z_m)^\alpha}{(z_m - z)^\alpha z_0} \right]^2 \right\} \right. \\ &\quad \left. \times \exp \left\{ -2 \left[\frac{x(z_m)^\alpha}{(z_m - z)^\alpha z_0} \right]^2 \right\} - \exp \left(-\frac{B^2}{2} \right) \right) \end{aligned} \quad (21)$$

From equations (20) and (21), the shear strain γ_{xz} in the x - z plane is given by

$$\gamma_{xz} = \frac{\partial u}{\partial z} + \frac{\partial v}{\partial x} = -\frac{As_m x(z_m)^\alpha}{(z_m - z)^{\alpha+2}} \times \left[\alpha(1 + \alpha) \left(\left\{ 1 - \frac{4\alpha}{1 + \alpha} \left[\frac{x(z_m)^\alpha}{(z_m - z)^\alpha z_o} \right]^2 \right\} \exp \left\{ -2 \left[\frac{x(z_m)^\alpha}{(z_m - z)^\alpha z_o} \right]^2 \right\} - \exp \left(-\frac{B^2}{2} \right) \right) \right. \right. \quad (22)$$

$$\left. \left. + \frac{4(z_m)^{2\alpha} (z_m - z)^2}{(z_m - z)^{2\alpha} (z_o)^2} \exp \left\{ -2 \left[\frac{x(z_m)^\alpha}{(z_m - z)^\alpha z_o} \right]^2 \right\} \right] \right.$$

The expression for engineering shear strain can be found by substituting equations (18), (19) and (22) into equation (10) to give

$$\epsilon_s = \frac{As_m(z_m)^\alpha}{(z_m - z)^{\alpha+1}} \left(\left[2\alpha \left(\left\{ 1 - 4 \left[\frac{x(z_m)^\alpha}{(z_m - z)^\alpha z_o} \right]^2 \right\} \exp \left\{ -2 \left[\frac{x(z_m)^\alpha}{(z_m - z)^\alpha z_o} \right]^2 \right\} - \exp \left(-\frac{B^2}{2} \right) \right) \right]^2 \right)^{0.5} \quad (23)$$

$$+ \left(\frac{x}{z_m - z} \left[\alpha(1 + \alpha) \left(\left\{ 1 - \frac{4\alpha}{1 + \alpha} \left[\frac{x(z_m)^\alpha}{(z_m - z)^\alpha z_o} \right]^2 \right\} \exp \left\{ -2 \left[\frac{x(z_m)^\alpha}{(z_m - z)^\alpha z_o} \right]^2 \right\} - \exp \left(-\frac{B^2}{2} \right) \right) \right. \right. \right. \right)^2$$

$$\left. \left. \left. + \frac{4(z_m)^{2\alpha} (z_m - z)^{2(1-\alpha)}}{(z_o)^2} \exp \left\{ -2 \left[\frac{x(z_m)^\alpha}{(z_m - z)^\alpha z_o} \right]^2 \right\} \right] \right)^2 \right)^{0.5}$$

NOTATION

- A* constant in displacement equations
- B* constant in displacement equations
- C* depth of tunnel cover
- D* tunnel diameter
- i* width of surface settlement trough
- i_z* width of settlement trough at depth *z*
- K* constant relating width of surface settlement to depth of tunnel
- K_z* constant relating width of settlement trough to depth of tunnel at depth *z*
- N_c* stability number
- s* surface settlement (vertical displacement at ground surface)
- s_m* maximum surface settlement
- s_u* soil undrained strength
- s_{uo}* undrained strength at ground surface
- s_{u,T}* soil undrained strength at level of centre of tunnel
- u* horizontal displacement
- V_s* volume of surface settlement trough (per metre length of tunnel)
- v* vertical displacement
- x* lateral displacement from vertical centreline of tunnel
- z* depth below ground surface
- z_m* depth below ground surface of point of intersection of extension of vertical boundaries of deformation mechanism with extension of vertical centreline of tunnel
- z_o* depth to centre of tunnel
- α* constant controlling vertical curvature of outer boundary of plastic deformation mechanism
- δv* vertical displacement increment
- γ* unit weight of soil
- γ_{xz}* shear strain in *x-z* plane
- ε_s* engineering shear strain
- ε_x* strain in horizontal direction (*x*-direction)
- ε_z* strain in vertical direction (*z*-direction)
- ρ* rate of change of undrained strength with depth
- σ_S* surface surcharge pressure
- σ_T* tunnel supporting pressure

REFERENCES

Attewell, P. B. (1978). Ground movements caused by tunneling in soil. *Proceedings of the international conference on large movements and structures* (ed. J. D. Geddes), pp. 812–948. London: Pentech Press.

Broms, B. B. & Bennermark, H. (1967). Stability of clay in vertical openings. *J. Soil Mech. Found. Div. ASCE* **193**, No. SMI, 71–94.

Chen, W. F. (1975). *Limit analysis and soil plasticity*, Developments in Geotechnical Engineering, 7. Amsterdam: Elsevier.

Clough, G. W. & Schmidt, B. (1981). Design and performance of excavations and tunnels in soft clay. In *Soft clay engineering* (eds E. W. Brand and R. P. Brenner), pp. 569–634. Amsterdam: Elsevier Scientific.

Davis, E. H., Gunn, M. J., Mair, R. J. & Seneviratne, H. N. (1980). The stability of shallow tunnels and underground openings in cohesive material. *Géotechnique* **30**, No. 4, 397–416.

Drucker, D. C., Greenberg, H. J. & Prager, W. (1952). Extended limit design theorems for continuous media. *Q. Appl. Math.* **9**, No. 4, 381–389.

Mair, R. J. (1979). *Centrifugal modelling of tunnel construction in soft clay*. PhD thesis, University of Cambridge.

Mair, R. J. (1993). Developments in geotechnical engineering research: applications to tunnels and deep excavations. Unwin Memorial Lecture 1992. *Proc. Inst. Civ. Engrs Civ. Engng* **97**, No. 1, 27–41.

Mair, R. J. & Taylor, R. N. (1997). Bored tunnelling in urban environment. *Proc. 14th Int. Conf. Soil Mech. Found. Engng, Hamburg* **4**, 2353–2385.

Mair, R. J., Taylor, R. N. & Bracegirdle, A. (1993). Subsurface settlement profiles above tunnels in clays. *Géotechnique* **43**, No. 2, 315–320.

Peck, R. B. (1969). Deep excavations and tunnelling in soft ground. *Proc. 7th Int. Conf. Soil Mech., Mexico City* **3**, 225–290.

Rankin, W. J. (1988). Ground movements resulting from urban tunnelling. *Proceedings of the conference on engineering geology of underground movements*, Nottingham, pp. 79–92.

Sloan A. W. & Assadi A. (1993). Stability of shallow tunnels in soft ground. In *Predictive soil mechanics*, Proceedings of the Wroth Memorial Symposium (eds G. T. Houlsby and A. N. Schofield), pp. 644–663. London: Thomas Telford.